q = volumetric flow rate
r = pore radius
R = radius of largest pore
$\hat{r}$ = particular radius within pore
S = saturation
T = time
v = velocity
V = average pore velocity
V_p = pore volume
$\tilde{V}$ = velocity along most probable path
X,Y,Z = displacements in the x, y, z directions

Greek Letters

α, β = parameters in radius distribution
ϕ = porosity
ψ = angle from y axis projected in xy plane
ρ,ζ,η = dimensionless coordinates
θ = angle from z axis
σ = surface tension
σ^2 = variance
τ = dimensionless time
μ = viscosity
ω = angle of wetting

Subscripts

T = time
Z = coordinate, z direction

LITERATURE CITED

1. Bear, J., *J. Geophys. Res.*, **66**, 1185 (1961).
2. Chandrasekhar, S., *Rev. Mod. Phys.*, **15**, 1 (1943).
3. Grane, F. E., and G. N. F. Gardner, *J. Chem. Eng. Data*, **6**, 283 (1961).
4. Evans, R. B., G. M. Watson, and E. A. Mason, *J. Chem. Phys.*, **35**, 2076 (1961).
5. Fatt, I., *Petrol. Trans. Am. Inst. Mining Engrs.*, **207**, 144 (1956).
6. Foster, R. N., and J. B. Butt, *AIChE J.*, **12**, 180 (1966).
7. Haring, R. E., M.S. thesis, Univ. Tulsa, Okla. (1961).
8. Harleman, D. R. J., and R. R. Rumer, *J. Fluid Mech.*, **16**, 385 (1963).
9. Hoogschagan, J., *Ind. Eng. Chem.*, **47**, 906 (1955).
10. Josselin de Jong, G., *Trans. Am. Geophys. Union*, **39**, 67 (1958).
11. Mood, A., "Introduction to the Theory of Statistics," McGraw-Hill, New York (1950).
12. Patel, R. D., and R. A. Greenkorn, *AIChE J.*, to be published.
13. Pearson, K., ed., "Tables of the Incomplete Beta-Function," The University Press, Cambridge, England (1934).
14. Perkins, T. K., Jr., and O. C. Johnston, *Petrol. Trans. Am. Inst. Mining Engrs.*, **228**, 70 (1963).
15. Petersen, E. E., *AIChE J.*, **4**, 343 (1958).
16. Purcell, W. R., *Petrol. Trans. Am. Inst. Mining Engrs.*, **186**, 39 (1949).
17. Saffman, P. G., *J. Fluid Mech.*, **7**, 194 (1960).
18. Satterfield, C. N., and T. K. Sherwood, "The Role of Diffusion in Catalysis," Addison-Wesley, Reading, Mass. (1963).
19. Scheidegger, A. E., "The Physics of Flow Through Porous Media," Macmillan, New York (1957).
20. Scheidegger, A. E., *J. Geophys. Res.*, **66**, 3273.
21. Wakao, N., and J. M. Smith, *Chem. Eng. Sci.*, **17**, 825 (1962).

Manuscript received May 10, 1968; revision received October 9, 1968; paper accepted November 4, 1968.

Birefringent Flow Visualization of Transitional Flow Phenomena in an Isosceles Triangular Duct

RICHARD W. HANKS and JAMES C. BROOKS

Brigham Young University, Provo, Utah

A flow visualization study was made with an optically birefringent solution of milling yellow dye in water flowing through a transparent duct of isoceles triangular cross section. The present data confirm a number of theoretical predictions concerning transitional phenomena in triangular ducts. One of the most interesting of these phenomena is the existence of a region of simultaneous laminar and turbulent flow in the duct. The present results, which agree with the theory, indicate an order of laminar and turbulent flow which is inverse to previous observations made with smoke filament tracings.

The phenomena associated with the transition from laminar to turbulent motion have been a subject of increasing interest to researchers in fluid mechanics since Reynolds (*1*) first performed his classical dye injection studies. The dye injection technique of Reynolds has since proved a tempting means of making visible the properties of flowing streams and for visualization of the properties of turbulent eddies in transitional flow (*2* to *9*). Although the method seems simple, it is not without its pitfalls.

This technique was used (*4*, *5*) in a series of studies performed with pipes and concentric annuli in which dye filaments were injected into a flowing water stream from a series of bent needle injectors.* As a result of these

J. C. Brooks is with the Fluor Corporation, Los Angeles, California.

* These injectors resembled a Pitot tube turned downstream. They consisted of hypodermic needle tubing having a 90° bend near their terminus with the bent portion extending downstream parallel to the duct boundary. Dye was forced through these tubes and into the flowing stream.

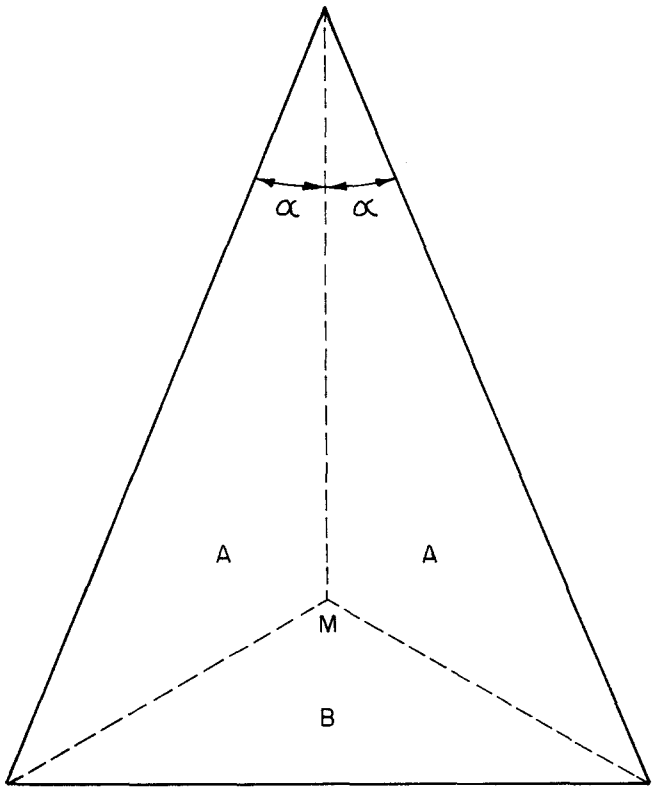

Fig. 1. Schematic representation of flow geometry for isoceles triangular duct. Points A and B are locations of regions of minimum stability.

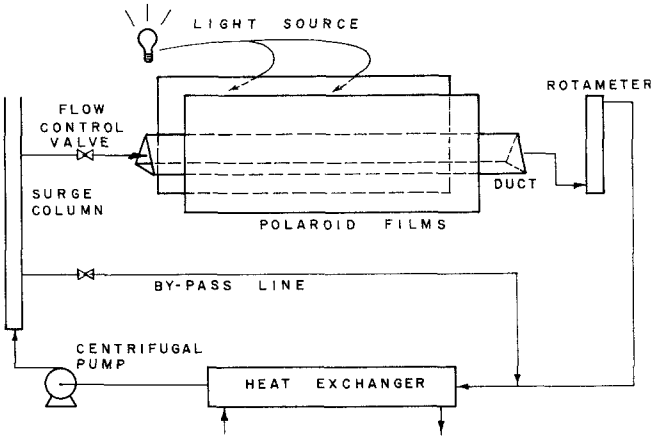

Fig. 2. Schematic diagram of flow system used to study probe influences on flow visualization.

dye injection flow visualizations, it was concluded that there existed a wave point Reynolds number, significantly smaller than the accepted critical Reynolds number of laminar-turbulent transition, at which a wavy disturbance in the flow was first observable. This disturbance always appeared first at the location of highest local velocity in the channel, and the disturbed zone spread outward toward the boundaries as the bulk flow Reynolds number increased above the wave point number. On the basis of this observation, the conclusion that turbulence was first observable at the location of maximum velocity was made. In contrast to these observations are those of Gibson (3) who observed by a dye filament technique* that for a pipe the flow was least stable at a point $r \simeq 0.58r_w$, where r_w is the pipe radius. This latter observation is in agreement with the theoretical prediction of Hanks (*10*) based upon the maximum rate of change of angular momentum of the fluid (*11*).

Lindgren (*12*) studied flows of optically birefringent suspensions of Bentonite in water and observed the influence of a conical probe protruding from the wall into the flow. This probe, which served simply as a source of disturbance, gave rise to a series of spiral vortices in its wake which closely resembled the dye patterns of Rothfus and Prengle (*4*). Lindgren (*12*) concluded that the observation (*4*) of wavy disturbances in dye filaments from probes inserted through the boundary was due merely to the probe disturbances.

* *In this experiment the dye stream was inserted into the flow field ahead of the carefully shaped rounded entrance to the pipe in the manner of Reynolds (1) rather than downstream from the duct entrance (4, 5).*

As a result of these criticisms, measurements of the wave point Reynolds numbers were made for a series of different diameter injection needles, and the data were extrapolated to zero needle diameter in an attempt to remove this effect. It is interesting to observe that for every point shown (5, Figure 2) in the plot of wave point Reynolds number vs. the ratio (needle diameter/pipe diameter) which was used to extrapolate to zero needle diameter, the Reynolds numbers for flow around the needle fall between 20 and 50, which is in the range where the familiar Von Karman vortex street develops.

In a more recent study, a similar arrangement was used (*6*) to introduce a smoke trace into a flowing air stream in two ducts of isosceles triangular cross section. On the basis of these observations, a series of conclusions concerning the nature of the flow in highly noncircular ducts were made (*6*). The present work (*13*) was performed to reexamine these conclusions which do not agree with recent theoretical predictions (*14*) for isosceles triangular ducts. In addition to reexamining the properties of the flow field in an isosceles triangular duct, the general effect of bent injection needles on a flow field was examined photographically to resolve the question raised but not solved by Lindgren (*12*).

THEORETICAL CONSIDERATIONS

Hanks and Cope (*14*) applied the stability theory of Hanks (*10, 11*) to the laminar velocity profile (*15*) for isosceles triangular ducts and were able to predict the occurrence of several rather unexpected phenomena during the transition process. Figure 1 is a schematic representation of the isosceles triangular cross section. Point M is the point of maximum velocity. Regions A are two symmetrically spaced and shaped regions of flow defined by lines drawn from M to the vertices of the triangle, and region B is an asymmetrically shaped region. Hanks and Cope's (*14*) calculations showed that regions A should become unstable to disturbances and undergo transition to turbulence at a mean velocity for which region 5 was still stable. This should occur at two symmetrically placed locations corresponding roughly to the placement of the letters A in Figure 1 so long as $\alpha < 30$ deg. When $\alpha > 30$ deg., the situation reverses and location B becomes unstable while locations A remain stable. The consequence of this prediction is that a range of Reynolds numbers is predicted to exist for which there will occur simultaneous regions of laminar and turbulent flow in such a duct. In particular, for the case $\alpha < 30$ deg., this theory (*14*) suggests that there will be a region of laminar flow in the

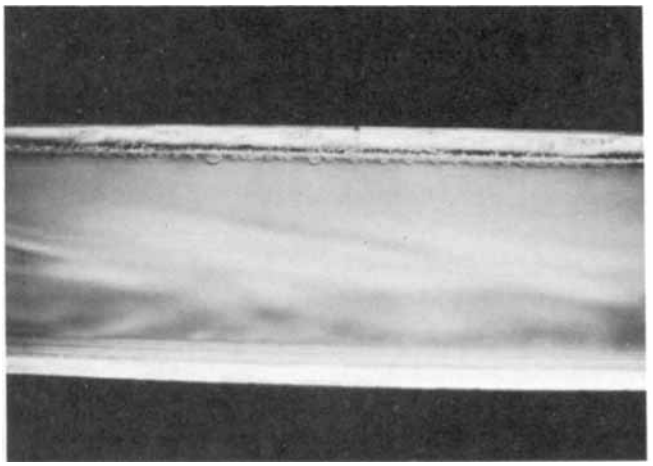

Fig. 3. Photograph of entrance region disturbed flow for $N_{Re} \doteq 1{,}300$.

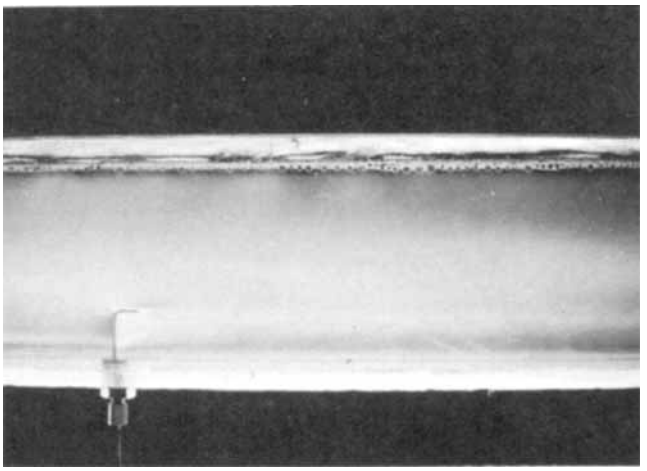

Fig. 4. Photograph of probe showing wake phenomenon in laminar flow. $N_{Re} \doteq 1{,}310$, and $x/L \doteq 0.7$ for probe tip.

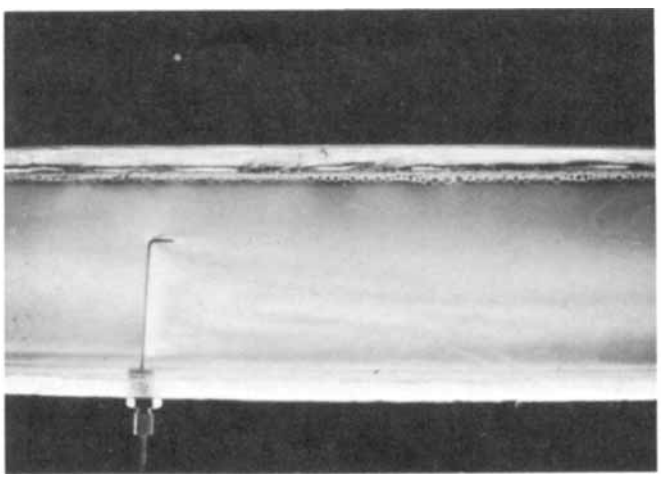

Fig. 5. Photograph of probe showing wake phenomena in laminar flow. $N_{Re} \doteq 1{,}310$, and $x/L \doteq 0.4$ for probe tip.

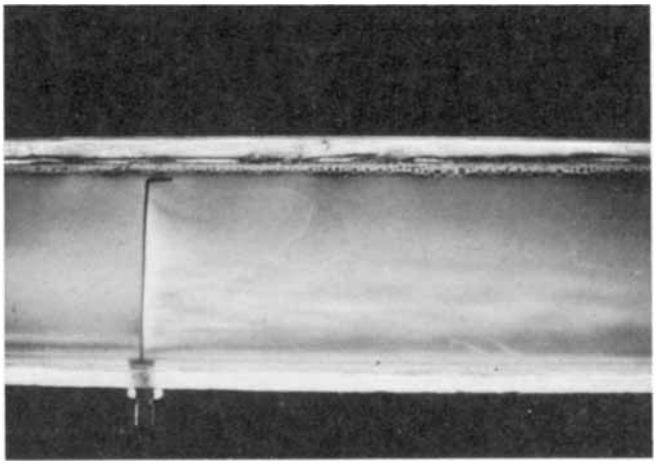

Fig. 6. Photograph of probe showing wake phenomena in laminar flow. $N_{Re} \doteq 1{,}310$, and $x/L \doteq 0.1$ for probe tip.

region B near the base of the triangle, while turbulence should occur in the two symmetric regions A near the apex of the triangle. Furthermore, for $\alpha = 12.4$ deg. [such as used previously (*6*) and in the present work (*13*)], no turbulence should be observed in fully developed flow at Reynolds numbers less than about 1,200. Finally, it would be expected that if regions A become turbulent first, there might be large turbulent disturbances generated in these regions which would probably penetrate entirely into the apex region despite the large damping effect of the converging walls (*6*).

EXPERIMENTAL APPARATUS

In order to study the flow in a triangular duct and to permit direct comparison with the above theoretical predictions and previous (*6*) conclusions, a triangular duct was constructed according to the specifications listed in Table 1. As can be seen, the experimental conditions of reference 6 were fairly closely duplicated. The fluid medium used in the present study was 1.4 wt. % solution of milling yellow dye in water. When used at 90°F., this particular solution was optically birefringent, had a specific gravity of 1.003, and had a viscosity of 9.1 centipoises.

The flow system used is illustrated schematically in Figure 2. It consisted of the Plexiglass test section fed from a small centrifugal pump and followed by a rotameter which permitted measurement of the flow rates. A heat exchanger preceding the pump permitted cooling water circulation to remove the pump energy input to maintain the temperature close to the 90°F. temperature which was found to be rather critical with respect to optical birefringence.

The Plexiglass test duct was placed between two crossed Polaroid sheets behind which was placed a uniform fluorescent light source. The polarized light thus generated caused the

Table 1. Specifications of Triangular Duct System Studied

	Present study	Reference 6
Apex angle, deg.	24.8	24.8
Hydraulic diameter, in.	1.075	0.901
Length, ft.	6.0	5.2
D_h/L	43	35
Reynolds number range	300-5000	500 to 8,000
Fluid used	Milling yellow sol'n.	Air
Visualization agent	Polarized light	Smoke
Probe diameter, in.	0.048	0.049
Probe length,* in.	0.44	0.55

* In direction of flow only.

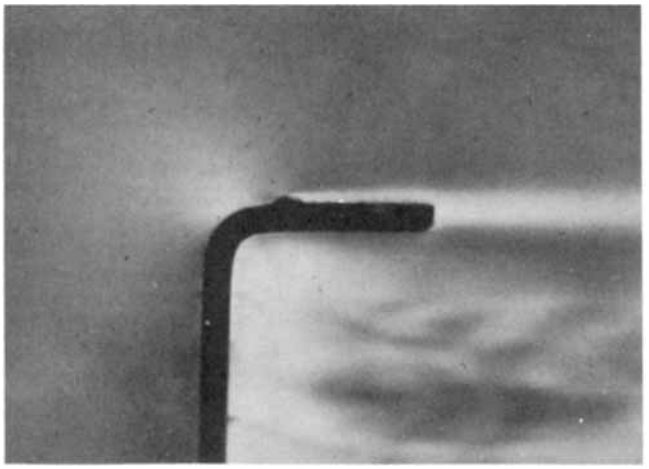

Fig. 7. Close-up photograph of probe tip for $N_{Re} \doteq 1{,}300$ and $x/L \doteq 0.6$ showing details of boundary layer and wake effects. Impinging flow to the left of the probe is laminar.

optically birefringent fluid to display stress patterns vividly in a variety of colors ranging from red to green. The intensity of the colors and their patterns varied with variations in the stress field, thus giving rise to a very vivid technicolor visualization of the flow field. Photographs were taken of the test section by viewing from the side opposite the light source. Black and white and color still shots were made as well as color movies of all the phenomena observed.

The probe used in the present study consisted simply of a piece of wire of the dimensions listed which was bent into the same shape as previously used (*4* to *6*) hypodermic needle injection probes and inserted through a Teflon seal plug in the duct base. The wire probe could be positioned manually in the duct cross section at selected positions along the altitude of the triangle.

Fig. 8. Close-up photograph of probe tip for $N_{Re} \doteq 4{,}000$ and $x/L \doteq 0.5$ with turbulent flow impinging from left. Note marked change in turbulence scale immediately behind probe.

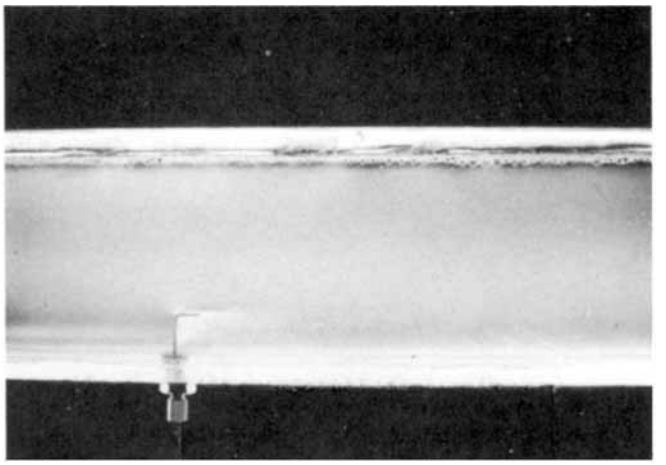

Fig. 9. Photograph of probe for $N_{Re} \doteq 1{,}000$ and $x/L \doteq 0.7$ showing effect of N_{Re} on wake behavior.

RESULTS

A series of pictures were taken of the duct section containing the probe wire at different heights above the base of the duct. The same series of probe heights was photographed at a series of Reynolds numbers ranging from 300 to slightly above 5,000.* Figures 3 through 7 are a typical series of such photographs taken at a Reynolds number of approximately 1,300. This series of pictures illustrates many of the effects which were observed. Figure 3 is a picture of the entry region of the duct showing the disturbed flow. This flow disturbance had been damped out by the time it reached the probe, as indicated by the uniform light density field preceding the probe in Figures 4 to 7.

Figures 4 to 6 illustrate the wake developed by the probe as a function of probe height x/L measured from the apex.† Several interesting features are evident in these pictures. Perhaps the most obvious feature is the pronounced disturbance in the wake behind the probe, whereas none is evident in the flow preceding the probe. The boundary layer which develops on the bent portion of the probe is clearly evident in Figures 4 and 5. A second feature of interest is the rather thick (about ¼ in.) layer of apparently undisturbed flow at the base of the probe. Careful study of Figure 4 reveals that immediately at the base of the probe this layer is thinner than elsewhere, as evidenced by the dip in the bright disturbance layer. At positions progressively downstream of the probe, the thickness of the dark layer of undisturbed flow increases significantly, indicating that the pronounced disturbance introduced by the probe has damped out. This is consistent with Hanks and Cope's (*14*) prediction of a stable laminar zone near the base of the flow for this Reynolds number range. For a duct of this apex angle, the maximum velocity occurs at $x/L \doteq 0.78$, which is slightly below the tip of the probe in Figure 4, and the point of minimum stability in region B occurs at about

* At about this level the calibrated scale of the rotameter was exceeded.

† This is the same measuring system used by previous workers (*6*). Thus, $x/L = 0$ corresponds to the apex of the triangle, while $x/L = 1$ corresponds to the base.

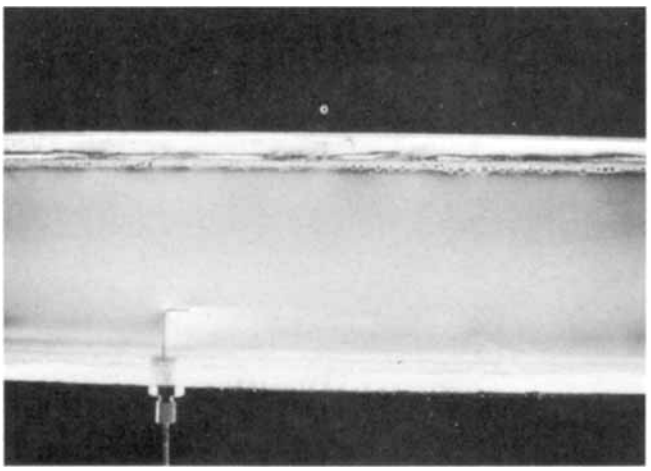

Fig. 10. Photograph of probe for $N_{Re} \doteq 1{,}150$ and $x/L \doteq 0.7$ showing effect of N_{Re} on wake behavior.

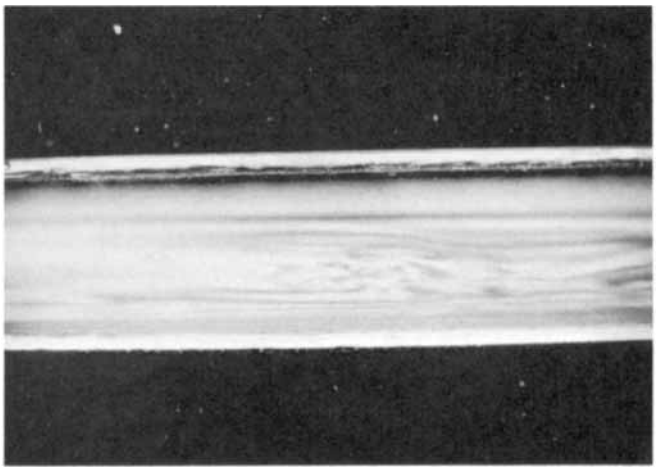

Fig. 12. Photograph of turbulent spot in upper region of duct for $N_{Re} \doteq 3{,}000$.

$x/L \doteq 0.9$. This latter point corresponds roughly to the initial bright dip at the base of the disturbance wake in Figures 4 to 6.

In Figure 5 the pronounced wake coming from the leading edge of the bent portion of the probe is very evident together with the continuous sheet of vortices being shed by the shank of the probe. Again, the marked damping of the disturbance near the base, indicating the intrinsic stability of that portion of the flow, is very evident. Another interesting feature of the wake behind the probe tip in Figure 5 is its diffuseness. Clearly, any dye or smoke trace introduced into such a wake would rapidly diffuse, losing its identity and leading one to the false conclusion that the flow being examined at that point is turbulent.

In Figure 6 the disturbance eddies, cast off most vigorously from the shank of the probe, do not interact with the laminar wake of the probe tip. From the form of the vortex sheet behind the probe shank, one would not expect interaction of these two wakes to occur until $x/L \simeq 0.3$.

That the flow impinging upon the probe is clearly nonturbulent is shown by Figures 7 and 8 which are close-up views of the probe at Reynolds numbers of 1,300 and 4,000, respectively. In Figure 8 the turbulence in the impinging flow is clearly visible, and the marked increase in turbulence due to the probe wake is plainly evident, while in Figure 7 the impinging flow presents a uniform light density field indicative of undisturbed flow. The details of the disturbance wake behind the probe in Figure 7 are very plain. The bright band showing the boundary layer on the bent portion of the wire and trailing diffusely off behind it was bright yellow in the color pictures. This is characteristic of a highly disturbed region of flow. The dark band immediately below it was deep red in color. The highly turbulent wake from the shank of the probe is very evident below the dark band.

Figures 9 to 11 show the probe at $x/L \simeq 0.7$, as in Figure 4, for Reynolds numbers of approximately 1,000, 1,150, and 1,500, respectively. These pictures illustrate clearly that the wake phenomenon is strongly dependent on the Reynolds number. In Figure 11, where the Reynolds number is approximately 1,500, the flow is just past the initial transition condition. Although the black and white photographs do not show it, the persisting inlet disturbance and eddying in the upper region of the duct is clearly visible as minor color fluctuations in the bulk stream at this point, indicating the disturbed nature of the flow. In Figure 11 this appears as a broad band of slightly brighter light intensity around and above the bent part of the probe.

In addition to the investigation of the influence of the probe on the flow visualization technique discussed above, a series of observations were made for disturbed and turbulent flows. It was of interest to examine the conclusions

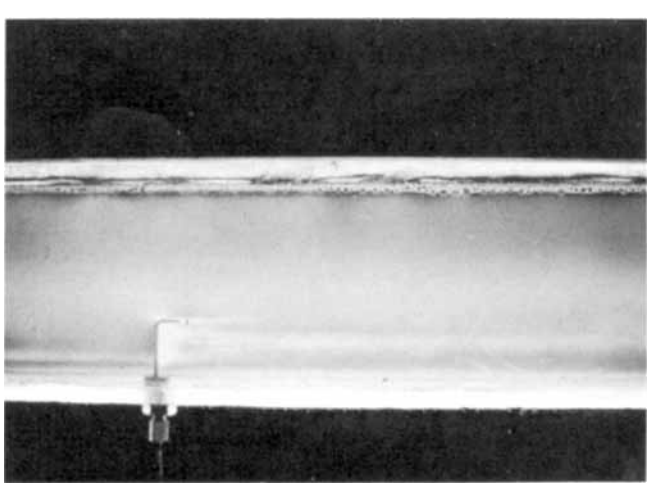

Fig. 11. Photograph of probe for $N_{Re} \doteq 1{,}500$ and $x/L \doteq 0.7$ showing effect of N_{Re} on wake behavior.

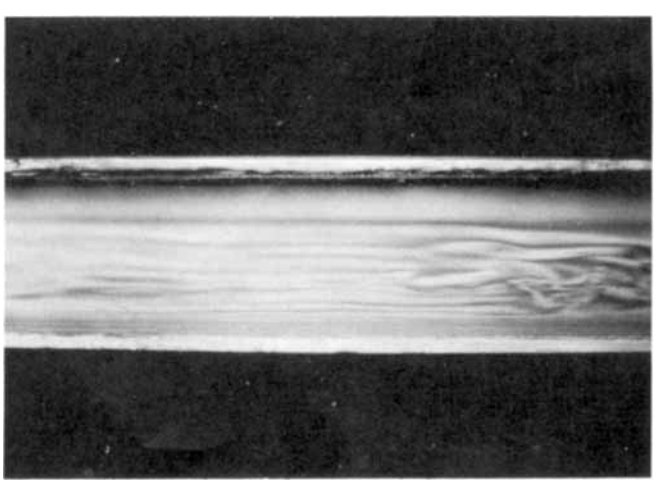

Fig. 13. Photograph of turbulent spot in upper region of duct for $N_{Re} \doteq 3{,}000$.

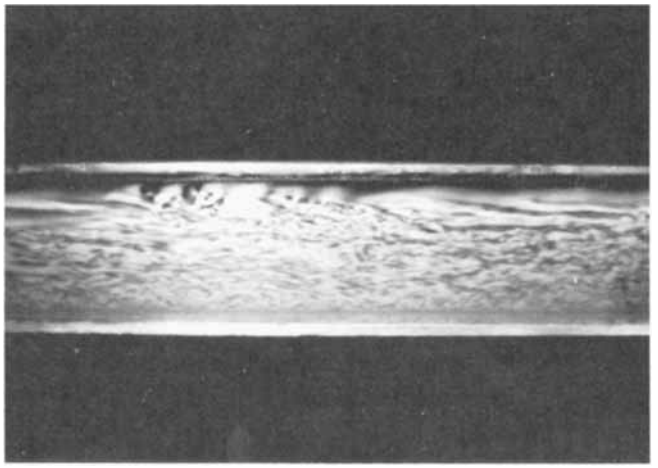

Fig. 14. Photograph of turbulent eddy penetrating apex region of duct for $N_{Re} \doteq 5{,}000$. Flow at this condition is fully turbulent.

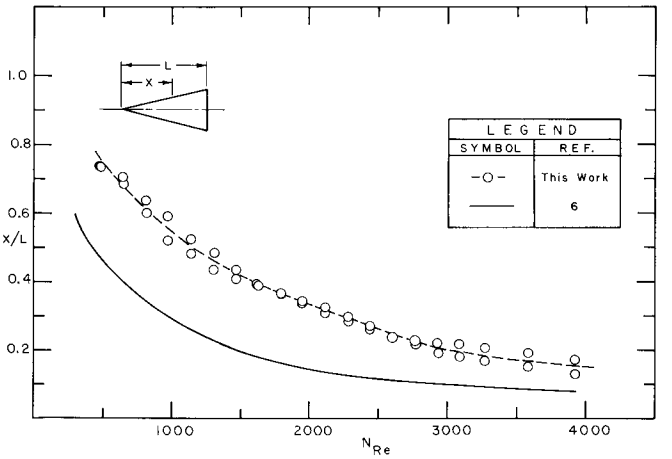

Fig. 15. Boundary curve delineating edge of laminar and turbulent zones in triangular ducts. Upper curve determined from present observations; lower curve from Eckert and Irvine (6).

made by Hanks and Cope (14) that turbulent eddies should be more readily generated in the upper region of the duct, and also the conclusion made by Eckert and Irvine (6) that "the damping properties of the shear flow near the triangle apex are so pronounced that they do not permit even the large turbulent fluctuations which are expected in the turbulent zone to spread into the corner region."

Figures 12 and 13 are photographs of the fully developed flow near the downstream end of the test section for a Reynolds number of approximately 3,000. The flow is clearly disturbed throughout as evidenced by the wavy stress lines in the field. In both of these photographs one can clearly see a large, energetic, turbulent spot similar to that described by Hama (7) and by Elder (8). From their location in the duct, these spots appear to have originated somewhere in the vicinity of $x/L \sim 0.5$ to 0.7 and from the side walls of the duct. Both observations are consistent with Hanks and Cope's (15) predictions for a duct of this apex angle. However, although these observations qualitatively verify the theoretical predictions (15), they are not quantitative, since no measurement of the actual point of instability is possible. Therefore, a more quantitative method of determining this point must be sought in future studies.

Figure 14 is a photograph of the fully turbulent flow for a Reynolds number a little greater* than 5,000. It is clear from this picture that a large, highly energetic, turbulent eddy has penetrated all the way up into the apex of the duct. This observation contradicts Eckert and Irvine's (6) conclusion, which was quoted in full above. Their result was probably caused by the distortion of the flow engendered by the proximity of the probe to the walls as it approached the apex of the triangle. This distortion of the flow in the apex by the probe, while not shown in any of the above photographs, was plainly visible in many of the exploratory observation runs which were made.

An attempt was made to determine the boundary curve (6) separating the apparent laminar and turbulent regions as observed previously (6). This was accomplished by setting the flow at a given Reynolds number and then adjusting the wire probe up or down until the bright yellow wake line behind the probe tip reduced to an arbitrarily selected size which was assumed to be non-disruptive had a dye stream been injected into it. At this condition it was arbitrarily assumed that a point on Eckert and Irvine's (6) boundary curve was defined.* The curve thus obtained is shown in Figure 15 together with the curve measured by the smoke tracer technique (6). It is clear that the qualitative behavior of the two curves is identical, the difference in level being quite probably due to the arbitrary cut off point selected* not being truly equivalent to that used by Eckert and Irvine (6).

DISCUSSION OF RESULTS

The results presented above and their interpretation present a picture of the phenomena associated with the laminar-turbulent transition in an isosceles triangular duct which agrees well with the theoretical model (14) but which disagrees with previous interpretations (6).

From Figures 7 and 8 it is clear that the present method can easily distinguish between laminar and turbulent flows. This being the case, Figures 4 to 6 clearly show that the introduction of a dye injection needle of the same shape as the present wire probe into the stream will introduce very pronounced disturbances into the flow. Furthermore, a dye stream introduced into the turbulent wake behind the probe tip would follow the fluctuations thereof, thus rendering them visible. In the absence of any means of making the impinging flow visible, one could thus be easily led to interpret the fluctuating dye pattern as turbulence. In terms of the wake of the probe, such an interpretation is correct, but in terms of the impinging stream, it is clearly incorrect for many situations, as Figures 4 to 7 show. In cases where the impinging stream is turbulent, as in Figure 8, the above interpretation would again be correct. However, the photographs here presented clearly show that the dye injection technique, when operated in this fashion (4 to 6), is incapable of distinguishing between a laminar or a turbulent impinging stream whenever the flow velocity is sufficient to result in the shedding of vortices from the probe. Therefore, we conclude that the description of a flow field as turbulent when based upon dye injection visualization (4 to 6) performed in

* The full capacity of the rotameter scale corresponded to a Reynolds number of about 5,000 and had been slightly exceeded in this run.

* This arbitrary choice was felt to be consistent with their criterion (6) of having no dispersion of their smoke trace. A color movie taken with the Polaroid camera lens rotated a great deal more than usual, however, showed fluctuations in the probe wake which were normally not seen with the usual Polaroid film in place. Thus, the curve in Figure 15 should probably be shifted significantly downward.

the above manner is at best highly questionable, and very probably incorrect. This conclusion is further substantiated by the curves in Figure 15. The data of previous figures confirm the fact that the impinging main stream is laminar for $N_{Re} < 1{,}300$ to 1,500. Therefore, the portion of the curve below this Reynolds number in Figure 15 is clearly fictitious as no turbulent flow exists, and all turbulent fluctuations observed (*6*) are due entirely to the probe wake. The similarity of the shape of the two curves strongly suggests that the remainder of the curve is likewise highly suspect. The difference in level (see previous footnote) suggests that the smoke filament (*6*) was actually more sensitive as a method of detecting the onset of wake formation behind the probe.

Figure 6 is very revealing in that it shows a region of undisturbed flow around the bent portion of the wire, while in the higher velocity region lower down the shank, the turbulent wake is very evident. This clearly indicates that a dye filament or smoke stream emerging from the bent tip would indicate a large laminar zone in the apex region with a turbulent zone near the base. Since the entire stream is in reality laminar (as evidenced by the uniform light density in Figure 6), this division into two zones is clearly incorrect. It would appear, therefore, that the previous (*6*) interpretation of the flow field in isosceles triangular ducts as consisting of two zones, one laminar and one turbulent, is either incorrect or, if correct, purely fortuitous.

Figure 14 clearly shows two important facts. It is evident that large turbulent eddies do, in fact, penetrate into the apex of the duct. This is contrary to previous conclusions (*6*) based on smoke studies at Reynolds numbers approaching 8,000. Clearly, the influence of the probe led previous workers to a questionable conclusion.

The turbulence intensity in the apex region appears to be decreased over that in the lower portions of the channel as evidenced by the lessening of the swirls in Figure 14 near the apex region. This observation appears to substantiate the previous observation (*6*) that the two walls in the apex region exert a marked damping influence. This conclusion is further supported by velocity profiles (*6*) measured with a Pitot tube. Unfortunately, these profiles were obtained at Reynolds numbers either completely below or completely above the transition region and hence cast no light on that interesting phenomenon.

From the photographic evidence presented herein, we may draw a number of conclusions concerning the nature of the transitional flow phenomenon in isosceles triangles and concerning the influence of a probe on flow visualization by dye or smoke injection.

Concerning the transitional flow phenomena in isosceles triangular ducts, we conclude that:

1. No turbulence exists in the flow stream for a bulk Reynolds number less than the critical value calculated by Hanks and Cope (*14*).

2. In the process of transition from laminar to turbulent flow, turbulence is initiated first in the apex region of the duct above the point of maximum velocity. This gives rise to a range of Reynolds numbers (relatively narrow) in which two separate stable zones of flow coexist simultaneously. The zone in the apex region (above the position of maximum velocity) is turbulent, while the zone near the base (below the position of maximum velocity) is laminar. This bifurcated flow regime is as predicted theoretically by Hanks and Cope (*14*). The previously reported dual zone (*6*) region was a result of the influence of the smoke injection probe on the flow and not the result of any physical phenomenon occurring in an isosceles triangular duct.

3. Although the converging walls of the apex portion of the duct do appear to exert a significant damping on the turbulence level of the flow in full turbulent flow, as suggested previously (*6*), turbulent fluctuations do penetrate all the way into the apex to a much greater degree than implied by previous workers (*6*). This penetration occurs with considerable regularity and frequency at Reynolds numbers as low as 4,000 to 5,000.

Concerning the influence of a dye iniection needle on flow visualization studies, we conclude that:

1. The technique of flow visualization, wherein dye or smoke is inserted into a flowing stream in the wake of an injection device of some sort which intrudes into the stream, is incapable of distinguishing fluctuations due to the probe wake itself from turbulence in the main stream which impinges on the injection device. Because of this insensitivity, previous workers (*4* to *6*) have been led to a series of apparently incorrect conclusions concerning the nature of transitional flow phenomena.

2. Previously reported (*4* to *6*) turbulent zones in high velocity regions of otherwise laminar flows (as manifested by frictional resistance measurements, velocity profiles, etc.) are merely observations of wakes generated by the dye or smoke injection devices.

3. Because of the long distances downstream from the probe over which the disturbances persist, it is highly questionable whether the placing of two such injection devices in tandem with each other to render the flow impinging on the downstream injector visible is any more reliable than using a single device.

4. Although the technique of flow visualization by dye or smoke injection in the wake of an injector may be useful in some applications, its use in studying transitional flow phenomena in a bulk stream appears to lead to spurious results and is therefore to be avoided. If dye or smoke injection is to be useful in studying transitional phenomena, it must be done according to a method such as used by Gibson (*3*), or by Hama (*7*), or by Elder (*8*).

ACKNOWLEDGMENT

This work was performed under the joint sponsorship of National Science Foundation Grant GK-1922 and a faculty research fellowship from Brigham Young University.

LITERATURE CITED

1. Reynolds, O., *Trans. Roy. Soc.*, **174**, 935 (1883).
2. Couch, W. H., and C. E. Herrstrom, thesis, Mass. Inst. Technol., Cambridge (June, 1924).
3. Gibson, A. H., *Phil. Mag.*, **15**, No. 7, 637 (1933).
4. Rothfus, R. R., and R. S. Prengle, *Ind. Eng. Chem.*, **44**, 1683 (1952).
5. *Ibid.*, **47**, 379 (1955).
6. Eckert, E. R. G., and T. F. Irvine, Jr., *Trans. Am. Soc. Mech. Engrs.*, **78**, 709 (1956).
7. Hama, F. R., *1960 Heat Trans. and Fluid Mech. Inst.*, p. 92 (1960).
8. Elder, J. W., *J. Fluid Mech.*, **9**, 235 (1960).
9. Runstadler, P. W., S. J. Kline, and W. C. Reynolds, *AFOSR Rept. MD-8*, Stanford University, Calif. (June, 1963).
10. Hanks, R. W., *AIChE J.*, **9**, 45 (1963).
11. *Ibid.*, **15**, 25 (1969).
12. Lindgren, E. R., *Arkiv Fysik.*, **12**, No. 1, 1 (1957). A preliminary part of this work appeared in *Appl. Sci. Res.*, **A4**, No. 4, 313 (1954).
13. Brooks, J. C., BES thesis, Brigham Young Univ., Provo, Utah (May, 1968).
14. Hanks, R. W., and R. C. Cope, *AIChE J.*, to be published.
15. Sparrow, E. M., *ibid.*, **8**, 599 (1962).

Manuscript received July 10, 1968; revision received October 30, 1968; paper accepted November 13, 1968.